

Simulating Ocean Surface Condition on an Extreme Weather Using Hydrodynamic 3D Model

Mahagnyana¹, Eko Hadi Sujiono², Pariabti Palloan³, Nayla Alvina Rahma⁴

(Received: 28 January 2024 / Revised: 6 February 2024 / Accepted: 9 March 2024)

Abstract— Research regarding sea surface condition during the coastal flood in Parepare 6 December 2021 has been carried out. In this research, the Delft3D model will be utilized to simulate the significant wave height (H_s) and direction, tide (η), and total water level (TWL) using input data from ECMWF ERA-5, including zonal (u) and meridional (v) wind, as well as surface air pressure data (p). The model's output demonstrate that the model is capable of accurately simulating the H_s and η , utilizing 2x2 gridded satellite data and the tide observation station of BIG, respectively. Hence, we conducted simulations to explore the interaction between H_s and η in the form of TWL in Parepare Bay, focusing in Bacukiki Barat and Ujung Districts on Desember 6, 2021. The results indicate that the maximum TWL for these two districts was 2.3376 meters dan 2.2096 meters, consecutively, both of which propagated towards the Parepare Coast. These extreme TWL height were exacerbated by the extreme rainfall occurring in Parepare City within 4-7 December 2021, which is exceeding 200 mm/day. The ECMWF ERA-5 model also revealed that the presence of strong winds blowing from The Java Sea to The Makassar Strait at speeds of around 25-30 knots, which is suspected to be the underlying cause of the high waves observed over the Makassar Strait.

Keywords— Parepare, coastal inundation, significant wave height, tide, total water level, extreme rainfall

I. INTRODUCTION

Parepare is a city located in the South Sulawesi Province of Indonesia, situated directly adjacent to the ocean. The city's geographical coordinates are 3.96-4.08 S and 119.60-119.72 E, with altitudes varying between 0 to 500 meters above sea level. Despite being bordered by the sea, Parepare features a predominantly hilly topography. According to the Indonesian Coastal Vulnerability Index Map issued by the Marine and Fisheries Research Agency, Ministry of Maritime Affairs and Fisheries of the Republic of Indonesia (2009), the coast of Parepare is classified as an area with low vulnerability. This classification indicates that the area is relatively resilient to coastal disasters. This low vulnerability is also supported by the latest research which suggests that the northern part of Parepare Bay exhibits low vulnerability [1]. The research is also stated that the northern part of the bay is characterized by volcanic rock and gravel sedimentation from the Bojo River and Karajae River.

On December 6, 2021, a coastal flood hit Parepare Bay at approximately 18:00 local time, resulting the inundation of residential properties. Reports indicated

that the coastal floods submerged multiple sub-districts, including Sumpang Minangae, Bacukiki Barat, and Ujung District. Due to the region's low coastal vulnerability, coastal flooding in Parepare actually is a relatively new phenomenon, particularly on the west coast of South Sulawesi. Coastal flooding can be caused by various factors. The most common cause of the coastal floods is coming from astronomical factors in the form of maximum tides. However, the maximum tides usually supported by another factor. Meteorological aspects, including high waves and extreme rainfall, could become dominant factors causing coastal floods, especially in Pontianak [2]. In Pontianak, the tidal flooding does not always occur during the maximum tide period. In fact, the tidal flooding may happen when extreme rainfall coincides with maximum tides as the extreme rainfall could inhibit the waters flowing from the rivers and overflow on land. Summarily, the heavy rain conditions can exacerbate the inundation in coastal areas [3].

In addition to meteorological and astronomical factors, the combination of the rise in Mean Sea Level (MSL) and land subsidence significantly influences the occurrence of coastal floods. Sea level rise can increase the potential for coastal flooding, especially in urban areas [4]. In addition, the escalation of the MSL also holds the potential to affect settlements and infrastructure damage and increase the sanitation and health problems. Furthermore, land subsidence that occurs in big cities is caused by excess ground-water extraction, soil characteristics in the form of alluvial soil, and construction loads [5], [6]. As happened in Jakarta and Semarang, land subsidence occurs at a rate of 3-10 cm/year and 14-19 cm/year, where these two locations are also affected by repeated coastal floods.

Among those several factors causing the coastal flood, storm surge is the most common cause [7]. A

Mahagnyana is with Department of Physics, Makassar State University, Makassar, 90224, Indonesia. E-mail: mahagnyana@bmkgo.go.id

Eko Hadi Sujiono is with Department of Physics, Makassar State University, Makassar, 90224, Indonesia. E-mail: e.h.sujiono@unm.ac.id

Pariabti Palloan is with Department of Physics, Makassar State University, Makassar, 90224, Indonesia.

Nayla Alvina Rahma is with Indonesia Meteorology Climatology and Geophysics Agency (BMKG), Maros, 90552, Indonesia. E-mail: naylaalvinar@gmail.com

storm surge can be described as the fluctuation in sea level, resulting from the effects of wind and shifts in air pressure over the oceans, induced by tropical storms [8]. Storm surge is caused by strong winds from a storm that are directed towards the coast, thus raising sea levels and triggering local extreme waves. The interaction between storm surge, peak tide, high waves, and increased river water discharge due to extreme rain, as a result of a storm, makes the potential for tidal flooding even worse. Nevertheless, due to the diminishing impact of the Coriolis force at latitudes nearer to the equator, Indonesia is comparatively less susceptible to disruptions from tropical storms [9]. In Indonesia, there will only be found the characteristics such as those found in tropical storms with a weaker intensity, such as strong winds, high waves, and extreme rainfall.

As the wave height plays an important role of a coastal floods, knowing the characteristics of wave, especially in the western waters of South Sulawesi and in Indonesia in general, is crucial. In general, variations of significant wave height (H_s) in Indonesian waters are largely determined by monsoon conditions, both of the Australian monsoon and the Asian monsoon [10]. The average H_s reaches its peak at the same time as the peak of the monsoon, as well as what happened in the western waters of South Sulawesi. The 10 years wave height average during the peak monsoon in the western waters of South Sulawesi is only 1 meter, which is categorized as slight sea. Meanwhile, the waves also propagate according to the monsoonal wind direction.

Research on coastal inundation has been widely carried out and is primarily dominated by the utilization of hydrodynamic models. The hydrodynamic model operates based on the principle of continuity, considering the flow characteristics of discharge and integrating internal flow simulation with the impact on fluid flow [11]. This model has found widespread application in the examination of tidal flooding cases, particularly in Indonesia [2], [12]. The Delft3D model is selected as the preferred model is grounded in its capability to account for the reciprocal effects of currents on waves, as well as the influence of waves on currents. Additionally, Delft3D has the capacity to calculate current movement in three dimensions Deltares [13], [14].

As it is known that Parepare Bay is an area that has low vulnerability [1], and it is also known that, climatologically, the wave height in the western waters of South Sulawesi has an average of only 1 m [10], hence, the combination between maximum tides and extreme waves is suspected to be the cause of the coastal flood. Therefore, in this research, we focused on simulating the H_s and η in Parepare Bay starting from 7 days before the incident, up to 7 days after the incident, to see the fluctuations of the H_s and η , as well as the interaction of these two parameters in the form of total water level (TWL). In addition, we also associate the results of the TWL simulation with the weather conditions at the incident, to see the potential of the extreme weather to exacerbate the inundation caused by the ocean condition.

II. METHOD

A. Model Description

The simulation in this study will be carried out using the Delft3D model. Delft3D is an integrated modeling program that can be used in multi-disciplinary approaches and 3D computation for wave and morpho dynamic modeling. Delft3D has several modules that can be used to run simulations such as water flow (Delft3D-FLOW), sediment transport (Delft3D-SED), waves (Delft3D-WAVE), water quality (Delft3D-WAQ and Delft3D-PART), and ecology (Delft3D-ECO) [14]. The Delft3D-FLOW and Delft3D-WAVE modules can be run either singly (offline) or simultaneously and interact with one another (online). This simultaneous simulation features are carried out by implementing data exchange between the two modules. The Delft3D-WAVE module recalculates the wave simulation results with the addition of input hydrodynamic data from Delft3D-FLOW and the new wave data can also be used as input data into Delft3D-FLOW [14]. This research will focus on the interaction between Delft3D-FLOW and Delft3D-WAVE which will be used in calculating H_s and η , and also estimating the TWL on the Parepare shoreline.

The Simulation Waves Nearshore (SWAN) third-generation wave model created by Delft University of Technology serves as the foundation for the Delft3D-WAVE module. In waters of deep, intermediate, and finite depth, the Delft3D-WAVE module can be used to calculate wave propagation, wave generation by wind, nonlinear wave-wave interactions, and dissipation for a given bottom topography, wind field, water level, and current field [13].

The wave action balance equation acts as the foundation for the Delft3D-WAVE model's prognostic equation. The spectral action balance equation, which is better suited for the utilization of numerical models in the presence of currents, describes how the wave spectrum evolves [15], [16]. The description of the equilibrium equation for wave motion in cartesian coordinates is explained in [17], [18]:

$$\frac{\partial}{\partial t} N + \frac{\partial}{\partial x} C_x N + \frac{\partial}{\partial y} C_y N + \frac{\partial}{\partial \sigma} C_\sigma N + \frac{\partial}{\partial \theta} C_\theta N = S_{in} \quad (1)$$

Where,

$$S(\sigma, \theta, x, y, t) = S_{tot} = S_{in} + S_{wcap} + S_{bot} + S_{br} + S_{nt} \quad (2)$$

The local rate of change in action density in time, shown by the first term in equation (1). The second and third terms (with propagation velocities of C_x and C_y in x and y space, respectively) illustrate the propagation of action in geographical space. The fourth term (with propagation velocity C_σ in σ space) denotes a change in relative frequency brought on by depth and current fluctuations. The fifth term, with propagation velocity C_θ in θ space, reflects depth-induced and current-induced

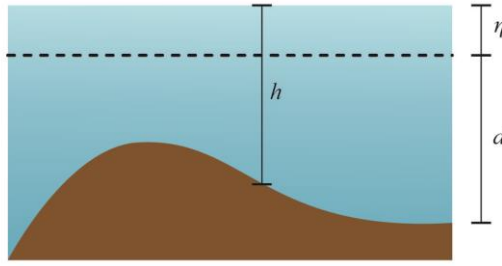


Figure 1. Description of Total Depth, h , depth according to reference level, d , and variation of the reference level, η

refraction. While at the right-side of the action balance equation represents the source of generation, dissipation, and non-linear wave-wave interactions. The first term on the right side (S_m) represents the transfer of wind energy to the waves, while the second, third, and fourth (S_{wcap} , S_{bot} , S_{br}) represent the dissipation of the wave due to the white-capping, bottom friction, and depth-induced breaking, respectively. The last term of the equation (S_{nl}) represents the non-linear wave-wave interactions.

Meanwhile, Delft3D-FLOW is a multi-dimensional (2D or 3D) hydrodynamic (and transport) simulation program that computes non-steady flow and transport phenomena as a result of tidal and meteorological stress on a rectilinear or a curved boundary fitted grid [14]. The Reynolds-Averaged Navier-Stokes (RANS) equations, which might be simplified for an incompressible fluid using the Boussinesq method and shallow-water assumptions, contribute to the basis of this module. Cartesian coordinates (x, y, z) must still be converted into σ -coordinates ($\tilde{x}, \tilde{y}, \sigma$) after the RANS equations have been made simpler (Broomans et al. 2003):

$$\begin{cases} \tilde{x} = x \\ \tilde{y} = y \\ \sigma = \frac{z-\eta}{d+\eta} \end{cases} \quad (3)$$

The following are the momentum equations in the corresponding x - and y - direction after transformation to σ -coordinates:

$$\frac{\partial u}{\partial t} + u \frac{\partial u}{\partial x} + v \frac{\partial u}{\partial y} + \frac{w}{H} \frac{\partial u}{\partial \sigma} = -\frac{1}{\rho_0} \left(\frac{\partial p}{\partial x} + \frac{\partial \sigma}{\partial x} \frac{\partial p}{\partial \sigma} \right) + f_v + F_x + \frac{1}{H^2} \frac{\partial}{\partial \sigma} \left(v'_h \frac{\partial u}{\partial \sigma} \right) \quad (4)$$

and

$$\frac{\partial v}{\partial t} + u \frac{\partial v}{\partial x} + v \frac{\partial v}{\partial y} + \frac{w}{H} \frac{\partial v}{\partial \sigma} = -\frac{1}{\rho_0} \left(\frac{\partial p}{\partial y} + \frac{\partial \sigma}{\partial y} \frac{\partial p}{\partial \sigma} \right) + f_u + F_y + \frac{1}{H^2} \frac{\partial}{\partial \sigma} \left(v'_v \frac{\partial v}{\partial \sigma} \right) \quad (5)$$

where h is the total water depth ($h = d + \eta$), d is the

water depth based on the datum, and η is the variation in water level as shown in figure 1. While F_x and F_y is the horizontal turbulent viscosity terms given by:

$$F_x = \left(\frac{\partial}{\partial x} + \frac{\partial \sigma}{\partial x} \frac{\partial}{\partial \sigma} \right) \tau_{xx} + \left(\frac{\partial}{\partial y} + \frac{\partial \sigma}{\partial y} \frac{\partial}{\partial \sigma} \right) \tau_{xy} \quad (6)$$

and

$$F_y = \left(\frac{\partial}{\partial x} + \frac{\partial \sigma}{\partial x} \frac{\partial}{\partial \sigma} \right) \tau_{xy} + \left(\frac{\partial}{\partial y} + \frac{\partial \sigma}{\partial y} \frac{\partial}{\partial \sigma} \right) \tau_{yy} \quad (7)$$

Where τ_{xx} , τ_{xy} , and τ_{yy} are the Reynold's stresses:

$$\tau_{xx} = 2v'_h \left(\frac{\partial u}{\partial x} + \frac{\partial \sigma}{\partial x} \frac{\partial u}{\partial \sigma} \right) \quad (8)$$

$$\tau_{xy} = v'_h \left(\frac{\partial u}{\partial y} + \frac{\partial \sigma}{\partial y} \frac{\partial u}{\partial \sigma} + \frac{\partial v}{\partial x} + \frac{\partial \sigma}{\partial x} \frac{\partial v}{\partial \sigma} \right) \quad (9)$$

$$\tau_{yy} = 2v'_v \left(\frac{\partial v}{\partial y} + \frac{\partial \sigma}{\partial y} \frac{\partial v}{\partial \sigma} \right) \quad (10)$$

In equations (4) and (5), u , v , and w are the time-averaged Reynolds components (mean flow) in the x -, y -, and z - directions, respectively, in σ coordinates. Unsteady acceleration is described by the first term in equations (4) and (5), while convective acceleration is described by the remaining terms. In the first and second terms, respectively, on the right side, the pressure, p , and the Coriolis effect are considered. Here, f stands for the Coriolis parameter, and it has the formula $f = 2\Omega \sin(\phi)$ where Ω is the magnitude of the earth's rotation vector and ϕ is the local latitude. On the other hand, the third and fourth terms introduce the horizontal and vertical turbulent viscosities, v'_h and v'_v , respectively, which imply Reynold's stresses.

B. Simulation Area and Period

The simulation of Significant Wave Height (H_s) and tides (η) in Makassar Strait (3.222–5.416 S and 115.88-

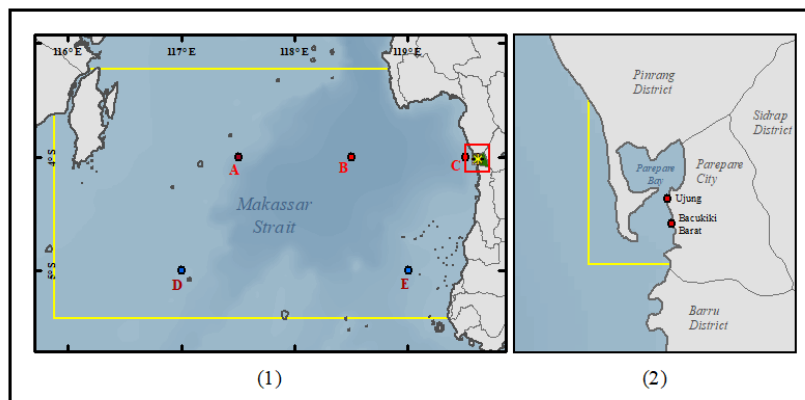


Figure. 2. The Location of A, B, C, D, And E Points in Makassar Strait (1) and the Location of Two Points in Parepare Bay (2). The Yellow Lines Are the Boundary of The Model in Each Location

119.675 E) and Parepare Bay (3.943-4.257 S and 119.568-119.649 E) is conducted from November 29, 2021, to December 13, 2022, as depicted in Figure 1. The Makassar strait H_S simulation aimed to understand the generation and propagation of sea waves influenced by the wind, with three observation points A (117.5 E and 4 S), B (118.5 E and 4 S), and C (119.5 E and 4 S). Subsequently, the research in the Parepare Bay location aimed to determine the η condition during the occurrence of tidal floods in Parepare on December 6, 2021.

The validation of H_S output is conducted at points D (117 E, 5S) and E (119 E, 5S) using the 2x2 gridded-satellite observation data. These points were selected due to the availability of the satellite observation data. Meanwhile, the η validation will take place at the Tide Observation Station of the Indonesian Agency for Meteorology, Climatology, and Geophysics (BIG) in the coast of Parepare City. Both parameter's validation is performed starting from December, 1 2020 to December, 31 2020.

C. Datasets

We generally divide the datasets into three groups: the geographical data, the validation, and the case. The geographical data consist of bathymetry data in Makassar strait with a resolution of 6-arcsecond (180 meters), the elevation data of Parepare City with a resolution of 0.27-arcsecond (8 meters), and tidal

constituent data from TPXO 7.2 Global Tides Model. The bathymetry and elevation data are provided by Indonesia Geospatial Agency (BIG). The validation and case data generally have the same parameters but different time period which the validation data from December, 1 2020 to December 31, 2020 and the case data from November 29, 2021 to December 13, 2021. We use 10-meter zonal (u) and meridional (v) winds and surface pressure (p) which are provided by European Centre for Medium-Range Weather Forecast Reanalysis v5 (ECMWF ERA5). Besides the atmospheric data, we also use the tides observation data that is obtained from Indonesia Geospatial Agency (BIG) and H_S 2x2 gridded-satellite observation data provided by Marine Copernicus. For the case period, we add rain observation data in Parepare City from Indonesia Meteorology Climatology and Geophysics Agency (BMKG) and spatial rainfall data from Global Satellite Mapping Precipitation (GSMaP) from December 4 to 6 2021.

D. Model Validation

We validate two main parameters of the model which are the and using the scatter plot, Root Mean Square Error (RMSE) and Coefficient of Correlation (R). The scatter plot is used to analyze the distribution of the observed and predicted data, while RSME and R are used to measure the model's performance in various field which satisfy:

TABLE 1.
 COEFFICIENT OF CORRELATION STRENGTH INTERPRETATION
 (HINKLE, D. E. ET AL. 2003)

Correlation Interval	Interpretation
0.00 – 0.30	Negligible
0.30 – 0.50	Low
0.50 – 0.70	Moderate
0.70 – 0.90	High
0.90 – 1.00	Very High

$$RMSE = \sqrt{\frac{1}{n} \sum_{i=1}^n (y_i - x_i)^2} \quad (11)$$

$$R = \frac{\sum (y_i - \bar{y})(x_i - \bar{x})}{\sqrt{\sum (x_i - \bar{x})^2 \sum (y_i - \bar{y})^2}} \quad (12)$$

where

- y_i = Observed value
- x_i = Predicted value
- \bar{y} = Mean observed value
- \bar{x} = Mean predicted value

the deterministic tide. η_{NTR} is simply defined as the difference between the observed tide and astronomical prediction tide. The last terms of the formula, the wave runoff, is the highest wave setup at the shoreline and often empirically related the deep-water wave height, wave length, and the slope of the beach [20]. The illustration of the terms in equation (13) can be seen in Figure 2.

F. Meteorological Analysis

The last analysis will be discussing about

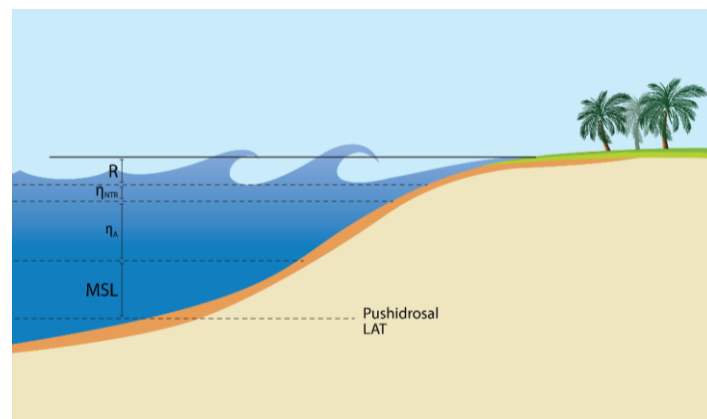


Figure 3. Definition Sketch of Total Water Level (TWL), MSL is the Mean Sea Level Which is Referenced to a Datum, in This Case We Use the Pushidrosal LAT. While η_A is the Delft3D-FLOW's Tide Prediction, η_{NTR} is the Change of the Water Level Apart from the Predicted Tide, and R is the Wave-Induced Change in Water Level (Serafin and Ruggiero, 2014).

Meanwhile, to interpret the strength of R , we used the guide as listed in Table 1.

E. Total Water Level Calculation

Furthermore, after analyzing the model's performance, we simulate the H_s and η from November, 29 2021 to December, 13 2021 over Makassar Strait and Parepare Bay which the location can be seen in Figure 1. The simulation is conducted 1 month before and after the incident to investigate the fluctuation and propagation of the H_s and η at point A, B, and C. Besides these three points, we also simulate the H_s and η over the Parepare Bay at the same period in two districts, which are Bacukiki Barat (119.622 E, 4.031 S) and Ujung (119.619 E, -4.013 S). After simulating H_s and η , we calculate the Total Water Level (TWL) using Serafin and Ruggiero's formula (2014):

$$TWL = MSL + \eta_A + \eta_{NTR} + R \quad (13)$$

Where MSL is the Mean Sea Level with respect to a datum. In this research, we use the MSL measured from the Lowest Astronomical Tides (LAT) issued by the Indonesian Navy's Center of Hydro-oceanography (Pushidrosal) with the height of 90 cm above the LAT. The next term, η_A , is the model's output which is predicted using the tidal harmonic constituents, while η_{NTR} is the change of the water level that is not related to

atmospheric factor which is closely related to the coastal inundation event on Parepare. We use the rainfall observation data from Indonesia Meteorology Climatology and Geophysics Agency (BMKG) which are located in Parepare City. We also compare the rainfall observation data with the Global Satellite Mapping of Precipitation (GSMaP) to analyze the spatial distribution of the rain as The Parepare City, topographically, characterized with hilly surface in the east side of the city, making the rain water runoff will flow to the lower area in the west coast of the city. We also plot the spatial distribution of the 10-meters wind speed and direction from the European Centre for Medium-Range Weather Forecast Reanalysis v5 (ECMWF ERA5) to evaluate how the wind forcing escalate the H_s and propagate to the low-lying coastal area in Parepare.

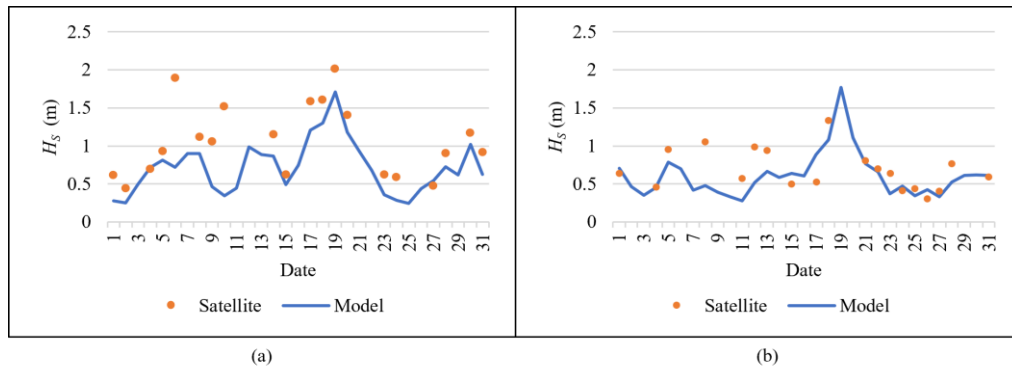


Figure 4. SWH Output from the Model Compared to Gridded Satellite Data at point D (a) and E (b)

III. RESULTS AND DISCUSSION

the model's output during December 2020. The gridded satellite observation data will be compared to the model's H_S output on point D and E. Meanwhile, the η output will be validated using the BIG's tide observation station on Parepare Bay on the same period as H_S .

Figure 4 shows the comparison between model's H_S output and gridded satellite data on point D and E. In this figure it can be seen that in general, the model has been able to simulate H_S conditions in the Makassar Strait properly, which is characterized by RMSE values of 0.4577 and 0.2349 at locations D and E, respectively. At location D, there are some observation data that can be categorized as outliers, such as on December 6 and 10 2020, which are characterized by values that are far apart from other data sets. There is also outlier data at location E, namely on December, 8 2020, but the value is not as noticeable as location D, so that the RMSE on E shows

We validate the Significant Wave Height (H_S) from better value than D. As we have mentioned above that the satellite data is a composite of other satellite data which is combined to form a grid data, so that there are several days where there is no observation data and also the possibility that there is biased data. Therefore, the use of observational data even though there are some outlier data cannot be avoided. Validation using longer observation data which is divided into several wave height categories is necessary for future research. Good results were also shown by the correlation coefficient on Figure 5. Although there are some data which far apart from their groups, the results still indicate that the model positively correlated with the satellite observation, which are indicated by R value of 0.740404 and 0.583352, coordinately at point D and E. At point D, we can see that most of the data distributed around the diagonal line, so that it got higher correlation than point E which the

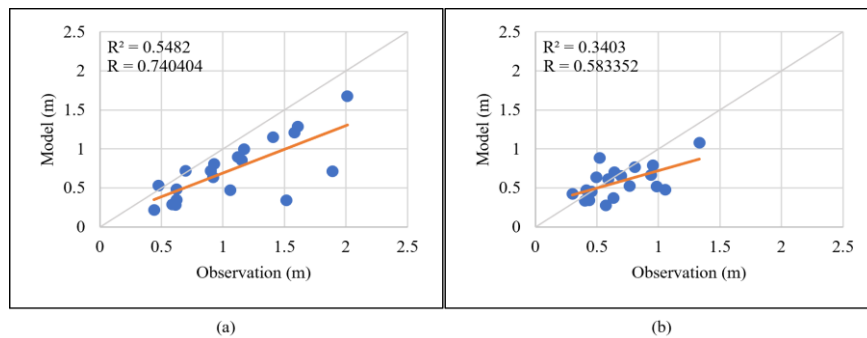


Figure 5. SWH Scatter Plot on Point D (a) and E (b) during December 2020

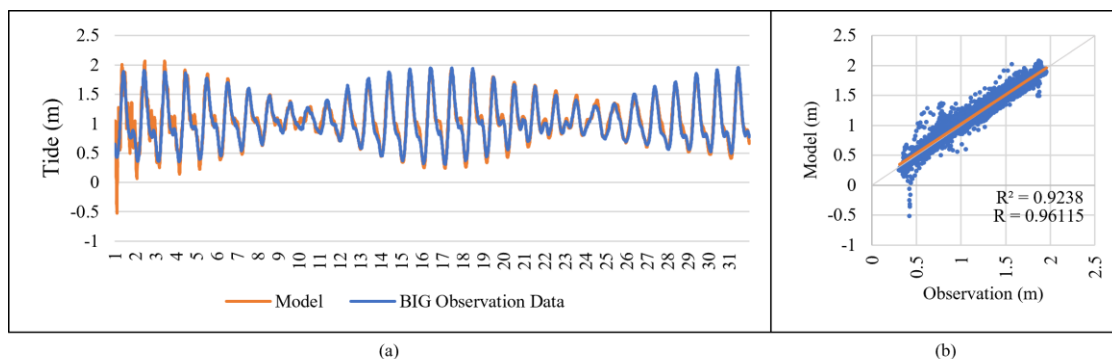


Figure 6. Model's η Output compared to BIG's Tide Observation Station Data during December 2020 in line (a) and scatter plot (b) graphs

data are more scattered. Moreover, from both Figure 4 and Figure 5, most of the data distributed below the diagonal line, which means that the model's estimation is tend to be lower than the satellite observation.

The next validation will be the model's η output, which is generated by harmonic prediction and validated using BIG's tide observation data during December 2020. Before we start to validate the model, we equalize the temporal resolution between these data, as the model's output is every 10 minutes while the observation itself is every 1 minute, hence, we are averaging the observation data in every 10 minutes. As we can see from Figure 6 (a), the first 5 days of simulation are the spin-up period which the model still needs time to reach an equilibrium state under the applied forcing. This

period is characterized by the unstable output of the model in the early running period, and then the model shows precise output for the rest of the period. However, although we include the spin-up period in the validation, the model can still predict the tide accurately with the RMSE value of 0.0107. This fine prediction is also indicated by the R value of 0.96115 which categorized as perfect correlation. From the scatter plot (Figure 6 (b)), the data distributed perfectly around the diagonal line. We also can consider that the data from spin-up period are located apart from the data groups, indicated by negative value in the scatter plot. Although we still include these data to the R calculation, we still get perfect R result.

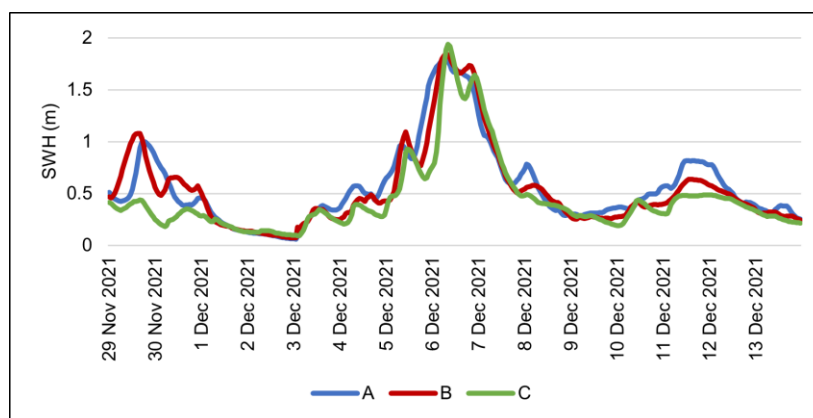


Figure 7. SWH Output from the Model at Location A, B, and C from November, 29 2021 to December,13 2021

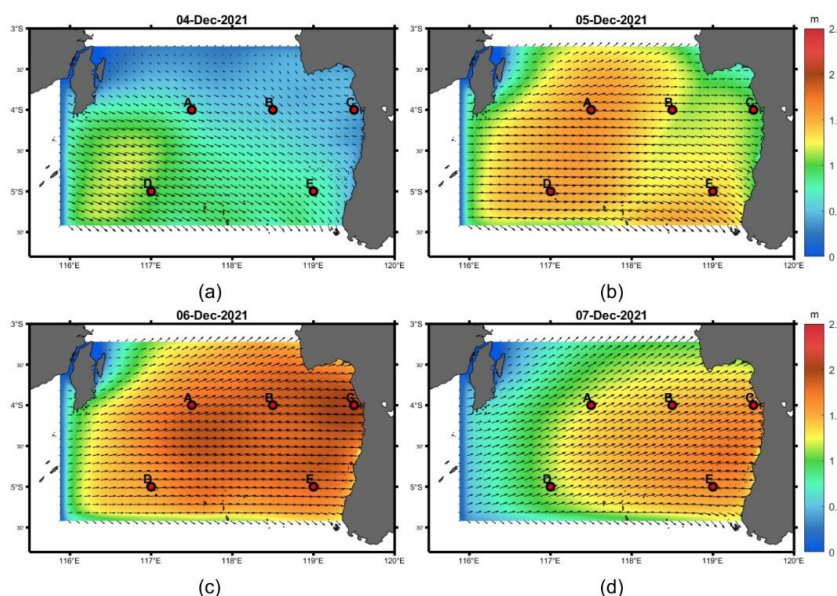


Figure 8. Spatial Distribution and Propagation of Daily Absolute SWH on December 4 (a), 5 (b), 6 (c), and 7 (d) 2021

After validating the model, we run the simulation 7 days before and after the coastal flood incident on December, 6 2021. As we can see in Figure 7, the H_S has a height of 0.5-1 meters at point A, B, and C in the early period of the simulation, and then it is declining until it reaches around 0.2 meters in December, 3 2021. The H_S starts to rise from December, 4 and hit its highest level on December, 6 2021 with a height of 1.81 meters, 1.85

meters, and 2.01 meter at point A, B, and C, respectively. This height occurs in all three points where point A has the lowest peak while point C has the highest peak. After reaching the highest H_S level, the height falls in the following days although it is still rising in the December, 11-12 2021. On Figure 8, we only highlighted the H_S from December, 4 2021 to December, 7 2021 as the H_S starts rising in 4th December, hit its top in 6th December,

and falling down in December, 7 2021. Based on the Figure, as the H_S propagates from west to east and reaches the west coast of South Sulawesi, its height is increasing as it is getting closer to land. The peak height of the H_S is able to propagate until it touches coastal areas, giving the potential for sea water to overflow towards land.

From Figure 7 and 8, we generally know that there is a significant rise of H_S in December, 6 2021 when the coastal floods incident happened. The next simulation will be focused in Parepare Bay, where the 2 locations were affected by coastal floods. From figure 9 (a) and (b), there is a significant rise of H_S in Parepare Bay at Bacukiki Barat and Ujung, as it also happens in Makassar Strait in the same day although the maximum height is lower. The significant rise of H_S occurs at the same time as the maximum η , leading to increase the maximum TWL height in December, 6 2021. If we take

a look at the H_S hourly, the maximum H_S in Bacukiki Barat is 0.4533 meters while in Ujung is 0.3374 meters, which both are occurred at 7 UTC and 8 UTC respectively. Meanwhile, the tide in Bacukiki Barat and Ujung is 1.9276 meters and 1.9142 meters, respectively, which occurs later than the H_S in 10 UTC and 11 UTC, correspondingly. The combination of these two parameters causes a significant increase of the TWL and reaches its maximum both at 10 UTC with 2.3376 meters at Bacukiki Barat and 2.2096 meters at Ujung. By the time that the maximum TWL happens in 10 UTC, the H_S is already declining slightly with 0.4099 meters at Bacukiki Barat and 0.3087 meters at Ujung. However, it still brings big impact to the TWL as the maximum tide hits its maximum at 10 UTC (Figure 9 (c) and (d)). The propagation of the TWL is also towards the shoreline (Figure 10), increasing the risk of coastal flooding as the sea water runoff.

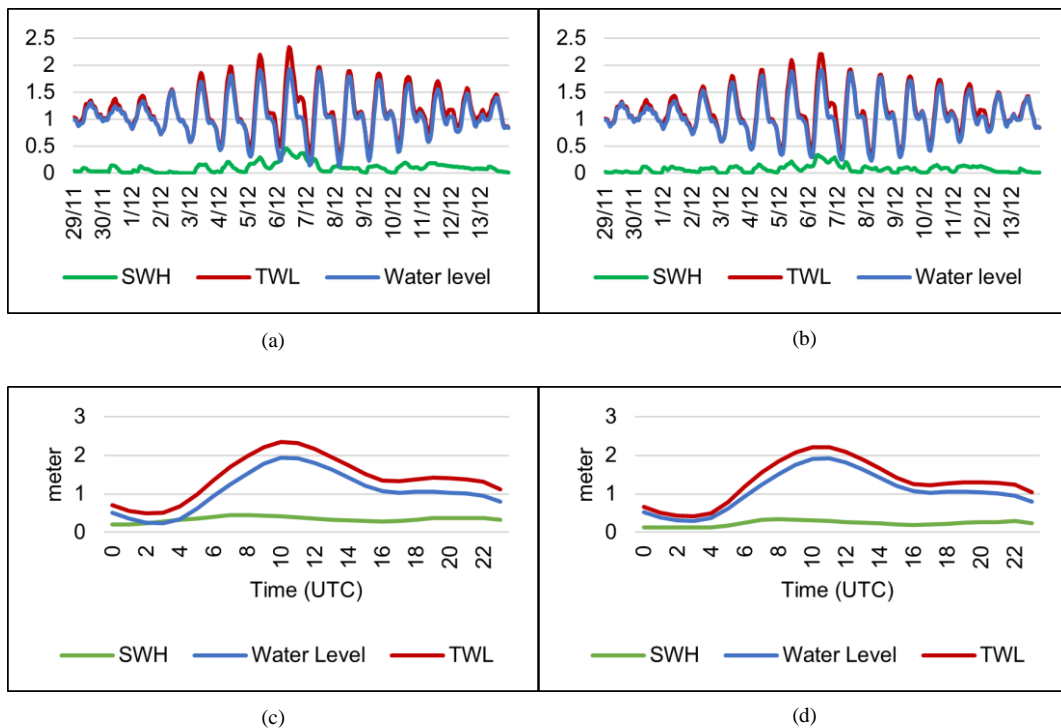


Figure 9. The Sea Surface Condition of Parepare Bay in Bacukiki Barat (A) and Ujung (B). The Two Graphs Below Them (C And D) are The Highlighted Period of These Two Locations Respectively in December, 6 2021

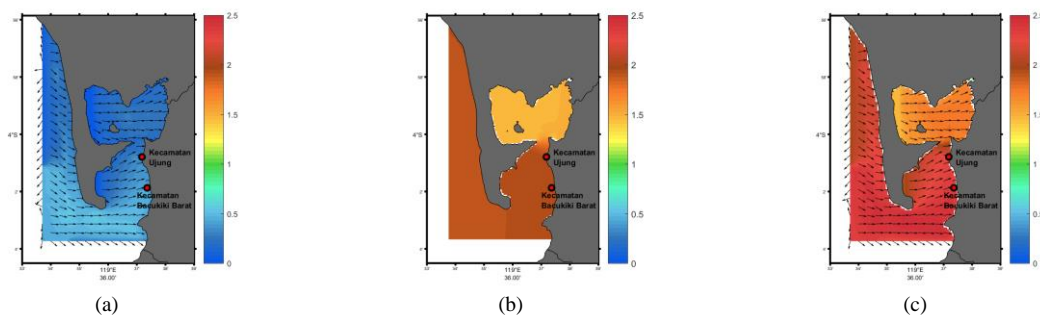


Figure 10. The condition of H_S (a), η (b), and TWL (c) over Parepare Bay on December, 6 2021 at 10UTC

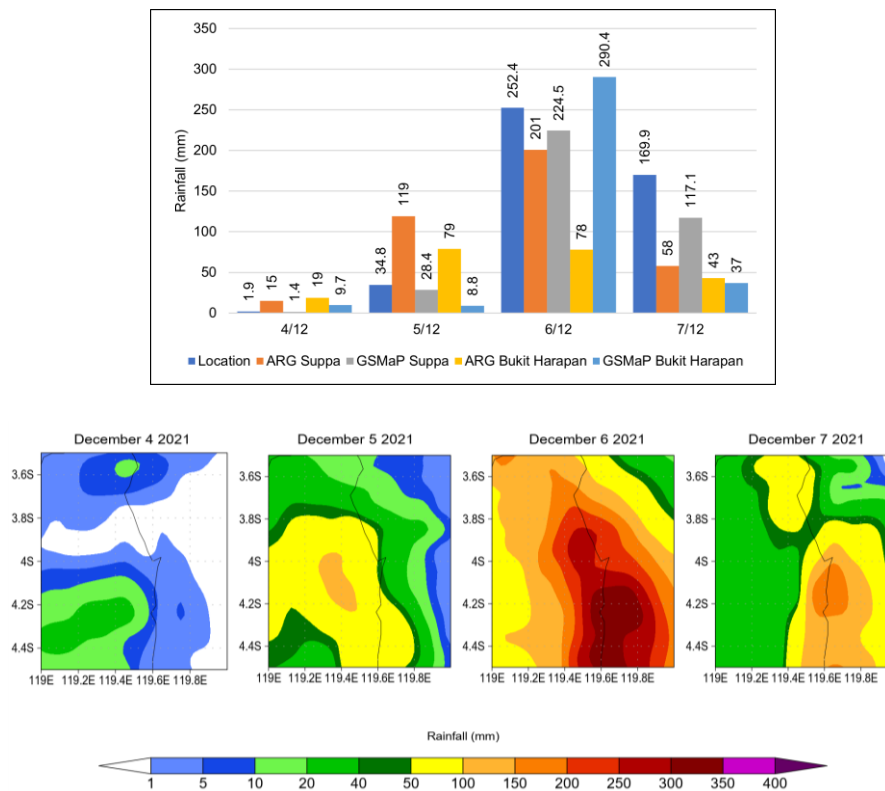


Figure. 11. The Rainfall on Parepare City and Its Surroundings from BMKG’s rain gauge and GSMaP Satellite on December 4-7 2021

Our next analysis will be focused on atmospheric condition that occurs on Parepare and its surroundings area. Hydrometeorological conditions are not the main cause of tidal floods, but they can exacerbate this phenomenon, so this analysis needs to be carried out. We analyzed the daily precipitation data from Global Satellite Mapping Precipitation (GSMaP) from 4th to 7th rainfall was also occurred in surrounding area of Parepare City. Apart from the satellite data, we also use automatic rain gauge (ARG) data from Agency for Meteorology Climatology and Geophysics (BMKG) at two locations in Parepare which are ARG Suppa and Bukit Harapan. Generally, the maximum rainfall in Parepare area was occurred on December 6 2021 that reached extreme intensity (>150 mm/day) (Figure 11). Furthermore, the maximum rainfall at ARG Suppa occurred on December, 6 2021 with 201 mm/day, while at ARG Bukit Harapan occurred on December, 5 2021 with 79 mm/day. The maximum rainfall data for the ARG Suppa is supported by GSMaP conditions which also have its maximum intensity on December, 6 2021 with a value of 224.45 mm/day. A different measurement was shown at Bukit Harapan which the GSMaP rain observation measured the rainfall value of 290.4 mm/day while ARG Bukit Harapan was only 78 mm/day. Even though there are differences in measurements between satellites and ARG, the rainfall at Bukit Harapan location is still categorized as heavy rain. Thus, the total rainfall in four days at Suppa location for the ARG and GSMaP

December 2021 and found that there is an increase in rainfall from 5th to 7th December 2021. The heavy rain was already occurred at 5th December with the rainfall of 50-100/day mm, and then it continued to increase with the rainfall of 200-250 mm/day. The following day was slightly decreased with the rainfall of around 100-150 mm/day. From figure 11, we can also consider that the satellite was 393 mm and 371.35 mm, respectively. Meanwhile at Bukit Harapan location, the ARG and GSMaP satellite was 219 mm and 345.9 mm, respectively.

Besides the rainfall, the atmospheric condition that we analyze is wind speed and direction. The wind speed is the main factor that generates waves over Makassar Strait. As we can see on Figure 12, there is a movement of wind speed with a speed of 25-30 knots moving easterly from the Java Sea on December 4 2021 and reaching the Makassar Strait on December 6 2021. In this case, the Java Sea and Makassar Strait are the wave generation areas (fetch) with a very wide area. Apart from that, the strong wind speed is persistent as it blows for several days. The impact of the large area of wave generation combined with persistent wind blowing times resulted in high waves in the Makassar Strait which headed towards the West Coast of South Sulawesi. We can have a direct relation from comparing Figure 8 and 13. The strong windspeed at December 4 2021 is still in the Java Sea and the wave height at Makassar Strait has not increased yet. When the strong winds enter Makassar

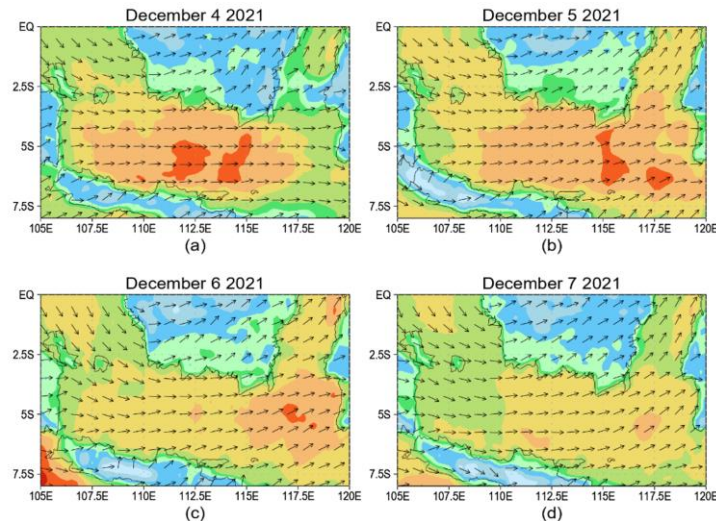


Figure. 12. The windspeed and direction over Java Sea and Makassar Strait on December 4 (a), 5 (b), 6(c), and 7 (d) 2021

Strait at December 5 2021, the H_S is increasing gradually and reaches its maximum height at December 6 2021 when the strong winds fully enter Makassar Strait. After reaching its maximum height, the SWH is declining in the last day after the strong winds dissipate because of the drag forcing with land.

Based on the results of the research above, the Parepare tidal flood event on December 6 2021 was started by the blows of the strong winds over Java Sea two districts in Parepare Bay (0.4533 meters and 0.3374 meters). However, this is not avoided Parepare Bay from the risk of coastal flooding due to high waves. Because, the high waves are coincided with the maximum tide level, causing the TWL to be able to overflow and reach land. The mechanism of the coastal floods often caused by the strong winds from a storm that could generate extreme waves that if the extreme waves are come along with the maximum tide, the risk of coastal flooding could even worse [7]. We do not have any storm because Parepare is located near the equator, but the strong winds could also be produced by another system such as monsoonal peak and Cumulonimbus clouds. Therefore, we have quite strong evidence that the Parepare coastal floods is dominantly caused by the extreme waves. Furthermore, the Parepare coastal floods is not only caused by the sea surface condition factor, but also exacerbated by extreme rain, thereby worsening the inundation at the location of the incident, slowing down the flow of water towards the ocean and increasing the height of inundation in coastal areas.

As for another possible cause of coastal floods such as like sea level rise and land subsidence which the characteristics of these two causes are mainly the repeated incident of coastal floods when the maximum tides happen. However, Parepare does not suffer from regular tidal floods, so that the coastal flood incident in Parepare does not caused by such factors as happened in Jakarta [21] and Semarang [22]. An area that composed by alluvial soil such as northern area of Java Island is vulnerable to land subsidence [5], [6]. If there is massive ground-water extraction and heavy construction loads over a coastal city, the subsidence could get even worse.

and Makassar Strait at December 4-6 2021. The persistent strong wind is combined with the fetch of the wave that stretches from the Java Sea to Makassar Strait is wide enough to generate high waves that could propagate eastward and reach the coast of Parepare City. Actually, the shape of Parepare Bay which facing south direction resulting the coastal area being protected from direct waves from Makassar Strait. This can be seen from the difference in H_S at point C (2 meters) and However, Parepare beach composed by volcanic rocks and igneous rocks and some part of the beach is composed by gravel and sand sediment from the Bojo and Karajae river [1]. From these reason, sea level rise and land subsidence factors are not significant. Ground-water extraction and construction loads seem less impactful too to the Parepare coastal floods as Parepare is also not a metropolitan city which has densely populated city that extract massive amount of ground-water and has heavy construction loads like Jakarta and Semarang in Java Island.

IV. CONCLUSION

The validation of the model's output both H_S and η shows a good performance from the model which is indicated by good RMSE and R score. Although there are some outliers in the satellite observation data, the RMSE and R still show good score, meaning that the model could simulate the H_S and η more accurately if we exclude the outlier's data. The model can be used to simulate the H_S and η condition both for analysis and forecasting purpose. Meanwhile for the sea surface condition, the coastal floods in Parepare significantly caused by an escalation of ocean waves initiated by strong winds blowing along the Java Sea to the Makassar Strait. The waves were coming simultaneously at Parepare Bay with the maximum tides, causing a substantial rise of TWL. Any other possible causes of coastal floods seem to be less impactful in this case.

ACKNOWLEDGEMENTS

We wish to acknowledge the Indonesia Agency for Meteorology Climatology and Geophysics (BMKG) for the Delft3D license and kindly help on the model building and problem solving. We would also like to acknowledge Makassar State University (UNM) for giving a good quality of group to conduct research and development. We also thank to the editors and reviewers for their valuable comments and suggestions to improve the quality of this research.

REFERENCES

- [1] H. Sirajuddin and B. Rivaldi, "Coastal morphodynamic and assessments of coastal vulnerability index in Parepare bay," IOP Conference Series: Earth and Environmental Science, vol. 419, no. 1, 2020.
- [2] Kuntinah, I. R. Nugraheni, and R. Ardianto, "The Simulation of Water Level Using Delft3D Hydrodynamic Model to analyze the case of coastal Inundation in Pontianak," Innovative Technology and Management Journal, vol. 4, pp. 32–44, 2021.
- [3] Y. Shen, M. M. Morsy, C. Huxley, N. Tahvildari, and J. L. Goodall, "Flood risk assessment and increased resilience for coastal urban watersheds under the combined impact of storm tide and heavy rainfall," Journal of Hydrology, vol. 579, no. 434, pp. 1–41, 2019.
- [4] M. A. Marfai, "Impact of Sea Level Rise to Coastal Ecology: A Case Study on the Northern Part of Java Island, Indonesia," Quaestiones Geographicae, vol. 33, no. 1, pp. 107–114, 2014.
- [5] H. Z. Abidin, H. Andreas, I. Gumilar, T. P. Sidiq, and Y. Fukuda, "Land subsidence in coastal city of Semarang (Indonesia): Characteristics, impacts and causes," Geomatics, Natural Hazards and Risk, vol. 4, no. 3, pp. 226–240, 2013.
- [6] H. Z. Abidin, H. Andreas, I. Gumilar, and I. R. R. Wibowo, "On correlation between urban development, land subsidence and flooding phenomena in Jakarta," IAHS-AISH Proceedings and Reports, vol. 370, no. November, pp. 15–20, 2015.
- [7] R. Gayathri, P. K. Bhaskaran, and F. Jose, "Coastal Inundation Research: An Overview of the Process," Current Science, vol. 112, no. 2, pp. 267–278, 2017.
- [8] N. S. Heaps, "Storm Surges," in Oceanography and Marine Biology: An Annual Review, 1967.
- [9] J. L. McBride, "Tropical Cyclone Formation," in Global perspective on tropical cyclones, 1995, pp. 63–105.
- [10] M. F. Islami, H. A. Rejeki, and A. Fadlan, "Aqua MODIS and altimetry satellite data utilization for determining the effective time and area of fishing in South Sulawesi," IOP Conference Series: Earth and Environmental Science, vol. 280, no. 1, 2019.
- [11] K. A. Serafin and R. Peter, "Journal of Geophysical Research : Oceans extreme value approach," Journal of Geophysical Research: Oceans, pp. 6305–6329, 2014.
- [12] P. . Sanjaka, S. Widada, and I. . Prasetyawan, "Pemodelan Inundasi (Banjir Rob) di Pesisir Kota Semarang Dengan Menggunakan Model Hidrodinamika," Jurnal Oseanografi, vol. 2, no. 3, pp. 353–360, 2013.
- [13] Deltares, User Manual Delft3D-WAVE: Simulation of short-crested with SWAN. Netherlands: Delft, 2021.
- [14] Deltares, User Manual Delft3D-FLOW: Simulation of multi-dimensional hydrodynamic flows and transport phenomena, including sediments. Netherlands: Delft, 2021.
- [15] N. Booij, R. C. Ris, and L. H. Holthuijsen, "A third-generation wave model for coastal regions 1. Model description and validation," Journal of Geophysical Research: Oceans, vol. 104, no. C4, pp. 7649–7666, 1999.
- [16] T. W. Hsu, J. M. Liao, S. J. Liang, S. H. Ou, and Y. T. Li, "A note on the derivation of wave action balance equation in frequency space," China Ocean Engineering, vol. 25, no. 1, pp. 133–138, 2011.
- [17] K. Hasselmann et al., Measurements of wind-wave growth and swell decay during the joint North Sea wave project (JONSWAP)., no. January. Deutsches Hydrographisches Institutes-Hamburg, 1973.
- [18] J. Willebrand, "Energy transport in a nonlinear and inhomogeneous random gravity wave field," Journal of Fluid Mechanics, vol. 70, no. 1, pp. 113–126, 1975.
- [19] P. Broomans and C. Vuik, "Numerical Accuracy in Solutions of the Shallow Water Equations," Technical University of Delft, 2003.
- [20] P. Ruggiero, P. D. Komar, W. G. McDougal, J. J. Marra, and R. Beach, "Wave Runup, Extreme Water Levels and the Erosion of Properties Backing Beaches," Journal of Coastal Research, vol. 17, no. 2, pp. 407–419, 2001.
- [21] M. A. Marfai, "Impact of coastal inundation on ecology and agricultural land use case study in central Java, Indonesia," Quaestiones Geographicae, vol. 30, no. 3, pp. 19–32, 2011.
- [22] M. A. Marfai and L. King, "Potential vulnerability implications of coastal inundation due to sea level rise for the coastal zone of Semarang city, Indonesia," Environmental Geology, vol. 54, no. 6, pp. 1235–1245, 2008.